DOI: 10.1002/masy.200851009

Bisthiol-Assisted Multilayers' Self-Assembly of Gold Nanoparticles: Synthesis, Characterization, Size Control and Electrocatalytic Applications

Ahmed I. Abdelrahman,[1] *Ahmad M. Mohammad,*[1,2] *Mohamed S. El-Deab,*[1,2]
Takeyoshi Okajima,[1] *Takeo Ohsaka**[1]

Summary: The layer-by-layer (LBL) approach has been utilized to self-assemble multilayers films of citrate-stabilized gold nanoparticles (AuNPs) on polycrystalline gold (poly-Au) substrates. 1,4-benzenedimethanethiol (BDMT) was used as a cross linker to bind every two successive AuNPs layers. The transmission electron microscopy (TEM), and X-ray photoelectron spectroscopy (XPS) techniques were employed to confirm the existence of the alternative layers of AuNPs and BDMT in the self-assembled multilayers film. The AuNPs modified poly-Au electrode showed a significant electrocatalysis towards the reduction of oxygen (a positive potential shift of about 100 mV was observed in the reduction peak potential compared to that obtained at the bare poly-Au electrode). The AuNPs tend to aggregate during their assembling to different extent which markedly depends on the substrate geometry and roughness. An effort was dedicated to understand and control the aggregation phenomenon.

Keywords: electrocatalysis; gold nanoparticles; hydrogen peroxide; layer-by-layer; oxygen reduction; self assembly

Introduction

Advances in nanotechnology are currently of a significant impact on several scientific fields, boosting the development of a variety of important technologies. The impact of these rapidly developing technologies is particularly significant in the electrochemical industry, where a number of nanoparticle-based arrays have been introduced for sensing and catalytic applications.[1,2] Among several reasons, the fascinating physical and chemical properties of metal and/or metal oxide nanomaterials are quite reasonable causes for the rapid progress in nanotechnology both in fundamental studies and technological applications. These includes the high effective surface area, catalytic activity, quantum confinement, etc.[3–8] Gold nanoparticles (AuNPs), in particular, attract a rapidly increasing attention due to their potential applications in electronics, optoelectronics, as well as chemical and electrochemical catalysis.[6,9,10] Several approaches have been proposed to assemble the AuNPs either chemically through an electrostatic or covalent immobilization or electrochemically on different substrates.[1,11–14] Yet, the chemical deposition approaches excel the electrochemical ones in the smaller average particle's sizes of the produced AuNPs. No doubt, the size shrinkage of AuNPs is expected to influence their physical and chemical properties.[15,16] The capture of metal nanoclusters through the coordination with anchored ligands such as thiol terminated organic molecules

---

[1] Department of Electronic Chemistry, Interdisciplinary Graduate School of Science and Engineering, Tokyo Institute of Technology, Mail Box G 1-5, 4259 Nagatsuta, Midori-ku, Yokohama 226-8502, Japan
Fax: +81-45-924-5489;
E-mail: ohsaka@echem.titech.ac.jp

[2] Department of Chemistry, Faculty of Science, Cairo University, Cairo, Egypt
E-mail: ahmad@chem-sci.cu.edu.eg

was early suggested Wang *et al.*[17,18] This concept (i.e., capturing by coordination) was further developed to use dithiol double-ended organic molecules which can be bound covalently to the metal substrate by one end while keeping the other end (with a free thiol terminal group) pointing to the solution phase to allow for the confinment of the small metal nanoclusters atop this organic layer.[19,20] As one of the interesting approaches to chemically self- assemble the AuNPs, the layer-by-layer (LBL) technique, the concept of which was developed for the construction of multicomposite films from aqueous solution[21,22], was proved facile and flexible for the preparation of super-structured arrays of 3-dimensional nanoparticles sturctures.[23–28] Nanoparticles films prepared by LBL exhibited an independent repeated electrochemical behavior for the electroactive Os^{3+}/Os^{2+} and Ru^{3+}/Ru^{2+} redox centers.[29] Olek et al.[30] have also used the LBL approach to prepare a high concentration of nanotubes with a homogeneous distribution within a polymer matrix. Moreover, the LBL technique could be used to fabricate well-designed structures of covalently-linked multilayers of metallic nanoparticles on (3-aminopropyl) trimethoxysilane (APTMS)-coated glass,[31] gold,[32] and indium tin oxide (ITO) substrates using different bisthiol crosslinkers[12]. These tailored nanoparticles-based structures were found to possess unique optical and spectroscopic properties.[33]

Recently, our group has investigated the electrochemical reduction of oxygen at AuNPs electrochemically deposited on different substrates.[13] These nanoparticles exhibited an extraordinary electrocatalytic activity towards oxygen reduction. Cystamine, and 1,4-benzenedimethanethiol (BDMT) have also been utilized to chemically immobilize AuNPs on poly-Au substrates.[34] A significant increase in the cathodic peak current and a 130 mV-positive shift in the cathodic peak potential have been observed,[34] indicating that the AuNPs modification resulted in a good electrical communication with the underlying electrode surface.

Herein, we report on the synthesis, characterization, size optimization and applications of 3-dimensional mono- and/or multilayer(s) of AuNPs self-assembled on the surface of gold electrodes of different roughnesses using the LBL approach and BDMT as a cross linker.

Experimental Part

Electrodes' Preparation and Pretreatment

Three different Au substrates were utilized, namely, polycrystalline gold (poly-Au), poly-Au with electrochemically (EC) deposited gold nanoparticles (EC-poly-Au), and atomically flat Au (111) single crystal electrodes. The Au (111) electrode was softly cleaned by successive sonication in acetone, ethanol, and deionized water. Conventional procedures were applied to clean the poly-Au electrodes ($\phi = 1.6$ mm). Typically, the electrodes were mechanically polished with emery paper (2000-grade), then with aqueous slurries of successively finer alumina powder (particle size down to 0.06 μm) with the help of a polishing microcloth. The electrodes were then electrochemical cleaned in N_2 saturated 0.5 M H_2SO_4 by cycling the potential between −0.2 and 1.5 V vs. Ag|AgCl|NaCl(sat.) reference electrode at scan rate of 10 V s^{-1} for 10 min or until the cyclic voltammogram (CV) characteristic of a clean Au electrode is obtained. The EC-poly-Au electrode was prepared by the electrochemical deposition of AuNPs onto the thus-cleaned poly-Au electrode by applying a potential step electrolysis from 1.1 to 0.0 V vs. Ag|AgCl|NaCl(sat.) reference electrode for 60 s in an acidic bath of 0.5 M H_2SO_4 solution containing 1.0 mM $Na[AuCl_4]$ and 100 μM I^- ions. Thus, AuNPs of average particle size of 10–20 nm were electrodeposited.[35–37] Then, the EC-poly-Au electrode was cleaned electrochemically to remove the adsorbed iodide ions.

Synthesis of a Multilayers Film of AuNPs

The detailed procedure to prepare the citrate-stabilized AuNPs' colloidal solution has been reported previousely.[38] Typically, 1 ml of 1% $NaAuCl_4$ was added to 90 ml of water at room temperature. After 1 minute of stirring, 2 ml of 38.8 mM sodium citrate was added. Subsequently, 1 ml of freshly prepared 0.075% $NaBH_4$ in 38.8 mM sodium citrate was added and the colloidal solution was stirred for 5–10 minutes and stored in a dark bottle at 4 °C. The average size of AuNPs in this colloidal solution was about 2.6 nm in diameter.[38] Assembling the BDMT layer on the Au substrate was done by soaking the cleaned Au electrodes in an ethanolic solution of 1 mM BDMT for one hour. The BDMT-modified Au electrodes were, subsequently, washed well with copious amount of ethanol and water, and then kept in the Au colloidal solution for 12 hr at room temperature to allow for the capturing of the AuNPs atop the BDMT monolayer. The thus-prepared electrodes were rinsed again with water before measurements. Hereafter the BDMT-modified Au electrodes will be referred as BDMT1 and AuNPs-anchored BDMT-Au electrodes will be referred as Nano1 (see Figure 1). The BDMT molecules are adsorbed on Au surface in a perpendicular orientation with the lose of one thiol proton.[39] At Nano1 electrode, the AuNPs are covalently bonded with the mercapto-terminal groups.

Fabrication of BDMT and AuNPs multilayers was done by repeating the above procedures (soaking in BDMT then Au colloidal solutions) times the number of layers needed. For example, to fabricate Nano10 the above procedure was repeated 10 times.

Electrochemical and Materials Characterization

The electrochemical measurements were performed in a two-compartment three electrode cell with a gold working electrode (diameter 1.6 mm), a Pt wire auxiliary electrode and an Ag|AgCl|NaCl(sat.) reference electrode. To investigate the oxygen reduction reaction, O_2 gas was bubbled for 10 min into 0.1 M phosphate buffered solution (PBS) (pH = 7.0) to ensure O_2-saturation, and

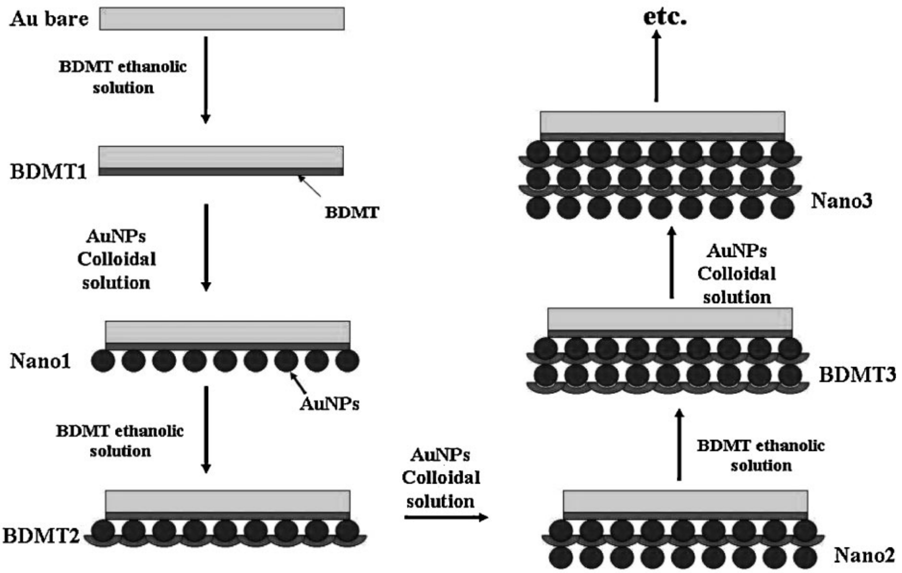

Figure 1.

A schematic illustration for the anchoring of the AuNPs from their colloidal solution on the BDMT (mercapto group-terminated self-assembled monolayer). (1) bare Au electrode is immersed in 1 mM BDMT ethanolic solution for 1 hr, and then (2) the BDMT-modified Au electrode is immersed in a colloidal AuNPs solution for 12 hr.

kept flowing over the solution during the measurements. The cyclic voltammograms (CVs) were recorded using a computer-controlled electrochemical analyzer CHI 604A. JEM-2010F analytical transmission electron microscope was used to capture the TEM images. The XPS spectra were recorded by ESCA3400 electron spectrometer (SHIMADZU) using an unmonochromatized X-ray source with Mg Kα (1253.6 eV) anode. Atomic force microscopic (AFM) image was obtained *ex-situ* using an AFM Nanoscale Hybrid Microscope VN–8000 — KEYENCE, in the direct contact mode. Note that the XPS and the AFM measurements were performed on planar Au substrates whereas the TEM imaging was performed on a Au mesh (2000-ppi grade). The Au meshs were prepared in a similar way to that employed for the planar poly-Au electrode except for the polishing step.

Results and Discussion

The Formation of BDMT and Au Nanoparticles Multilayers

Parts A-C of Figure 2 show the typical TEM images of Nano1, Nano2, and Nano10 mesh electrodes after immobilzation on poly-Au substrate. One can easily estimate the layers and their average thickness. In Figure 2A, one can almost see a uniform single layer of AuNPs with few uncovered sites on the mesh electrode surface.

According to this image, the average thickness of this layer is about 5.5 nm. Recalling the original average size of AuNPs in the colloidal Au solution before immobilization on the BDMT layer was 2.6 nm,[38] it can easily be anticipated that two or more Au nanoparticles were aggregated during their immobilization process atop the BDMT layer. This aggregation process is worthwhile to be investigated in order to identify its reasons and consequently to control it. This might be done to prepare well-designed AuNPs cluster arrays with the prospective size for a target application. Figures 2B and C show TEM images for the Nano2 and Nano10 electrodes, respectively. The average thickness of layers in these images is 10–11 nm and 50–60 nm for Nano2 and Nano10, respectively. This confirms the formation of 2 and 10 layers, respectively, each of which has a thickness of (ca. 5.5 nm). Therefore, the TEM investigation could ascertain the formation of successive AuNPs' layers. However, unfortunately, the investigation could not show clearly the distance between two successive AuNPs' layers. In fact, this distance corresponds to the length of the BDMT molecule, which is very short (0.8 nm),[40] a length that is very difficult for any imaging technique to detect.

The XPS measurements were then carried out to confirm the confinement of BDMT in-between the AuNPs' layers. Selected XPS measurements were taken for BDMT4 and Nano4 electrodes. The

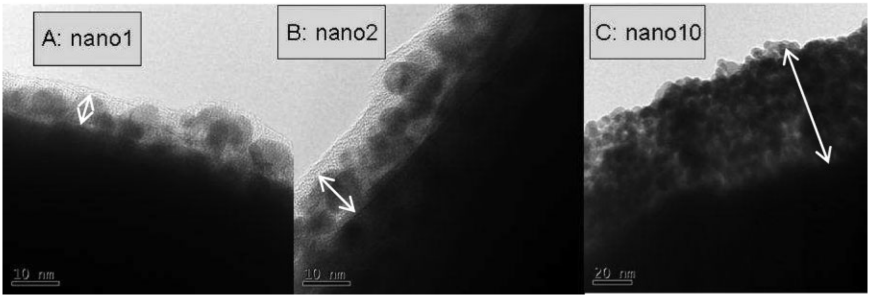

Figure 2.
TEM images for (A) Nano1, (B) Nano2, and (C) Nano10. The arrows indicate the AuNPs layers. See Figure 1 to identify the abbreviations.

spectra in both cases showed a broad band in the range 160–164 eV, in agreement with a previous finding for the S2p peak.[41] On the other hand, the S2p peak area of BDMT4 was relatively larger than that of Nano4, as in the case of Nano4, the BDMT layer lies beneath the AuNPs-layer, whereas in the BDMT4 the BDMT is a surface topmost layer. As well known, XPS is a surface technique, *i.e.,* surface topmost layers contribute more for photoemission signals than deeper layers. This proves the existence of BDMT layer as a covalent cross linker between the AuNPs layers.

Electrochemical Results

The electrocatalytic activity of the AuNPs' layers towards the reduction of oxygen has been examined in O_2-saturated 0.1 M PBS solution. Figure 3 represents the CVs obtained for the reduction of oxygen at (a) bare, (b) BDMT1, (b′, dotted line) Nano1, (c) BDMT2, (c′, solid line) Nano2, and (d, dashed line) Nano10 electrodes in 0.1 M O_2-saturated phosphate buffer solution (pH 7.0). Potential scan rate: 100 mVs^{-1}. The 2-electron reduction of oxygen to hydrogen peroxide at the poly-Au electrode occurred at around −0.22 V (Figure 3a), while the BDMT1 electrode did not show any voltammetric response for the reduction of oxygen within the employed potential window (Figure 3b). We suppose that the hydrophobic nature and compactness of the BDMT monolayer, and/or the shortage of $H^+(H_3O^+)$ near the BDMT monolayer are behind this behavior of oxygen reduction on BDMT1. Proceedings the reaction through either an inner sphere or outer sphere mechanism may also contribute. It is believed that the outer sphere mechanism is open to all redox active systems, while inner sphere mechanism, which is likely the mechanism for the oxygen reduction, requires the substitution of labile reactants and products.

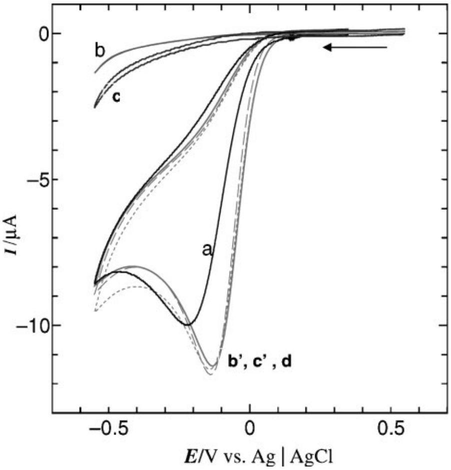

Figure 3.
CVs obtained for the oxygen reduction at (a) bare, (b) BDMT1, (b′, dotted line) Nano1, (c) BDMT2, (c′, solid line) Nano2, and (d, dashed line) Nano10 electrodes in 0.1 M O_2-saturated phosphate buffer solution (pH 7.0). Potential scan rate: 100 mVs^{-1}.

At Nano1 electrode, a well-defined wave for the reduction of oxygen was observed at −0.12 V, which is 100 mV less negative than that obtained at the poly-Au electrode, implying that the immobilized Au nanoparticles efficiently catalyze the reduction of oxygen. The sharp cathodic peak associated with an enhancement in the peak current reflects a fast electron transfer kinetics at the Nano1 electrode. The reduction process was proved to be diffusion-controlled at the nanoparticle-immobilized electrode, as evidenced by the linear increase of peak current with the square root of potential scan rate.[34]

Interestingly, there was no response for the reduction of oxygen, after assembling the second BDMT layer (BDMT2 electrode, Figure 3c). The second AuNPs' layer (Nano2) restored the catalytic activity towards the oxygen reduction (Figure 3c′). This behavior (i.e., losing of the electrocatalytic activity for oxygen reduction on BDMT monolayers and restoring it over AuNPs monolayers) has repeated for all the next layers as a zigzag response up to 20 alternative layers of BDMT and AuNPs (10 layers for each). It is interesting that the response for the oxygen reduction is completely suppressed when BDMT is assembled as a topmost layer, while a renewed-electrocatalytic response is obtained at the AuNPs' modifies electrode (see Figure 3d for

Nano10). Further work is required to understand the nature of the electron transfer through the layers.

AuNPs' Aggregation

The TEM images (shown in Figure 2) inferred that few AuNPs aggregated during the anchoring process. This kind of aggregation has not been observed in the colloidal solution due to the strong stability of the negatively charged AuNPs by the citrate shield. A considerable attention is being paid in the literature to clarify and control the aggregation phenomena of AuNPs in the solution phase.[10,38,42] On the other hand, when AuNPs are immobilized on solid substrates, several factors are believed to influence the extent of their aggregation. Some of these factors are related to the substrate and others to the binder and/or stabilizer. The influence of the substrate roughness on the extent of aggregation has been investigated. Thus, AuNPs have been chemically immobilized on smooth Au (111) and rough EC-poly-Au electrodes using BDMT as a cross binder. The electrodeposition of AuNPs on a poly-Au substrate was done to increase the roughness of the electrode. The TEM image in Figure 4 shows the morphology of the AuNPs after their chemical immobilization onto the EC-poly-Au substrate. Interestingly, a smaller average size (4.0 nm) was obtained for the chemically-anchored AuNPs (zone C). This means that the aggregation of the AuNPs occurred at a lesser extent than the case of the poly-Au electrode (see Figure 2A).

Immobilization of AuNPs was next performed on a smooth Au substrate with smaller roughness factor (i.e., single crystalline Au (111) substrate) and the sample was pictured by AFM (data are not included). Surface investigation of the this sample revealed a thickness of 8.2 nm for a one AuNPs layer, i.e., a higher extent of aggregation occurred during the anchoring process onto the Au (111) than that on the poly-Au. Hence, these results confirmed that decreasing the substrate roughness increases the extent of aggregation. We believe that the substrate roughness may influence the extent of aggregation, at least, through changing the surface coverage of the binder. Further investigation will be necessary to completely understand and control the aggregation phenomenon.

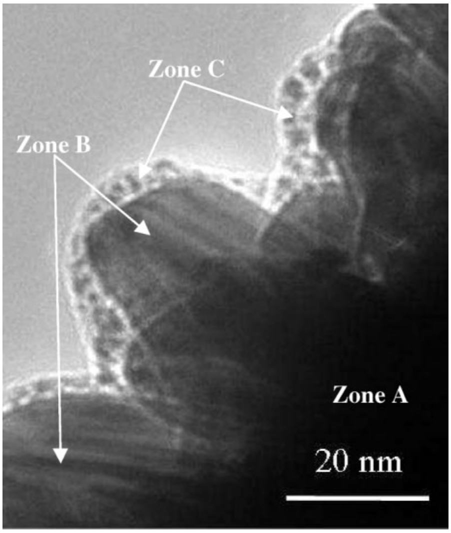

Figure 4.
TEM image for the AuNPs chemically immobilized on EC-poly-Au substrate. Zones A, B and C are, respectively, for poly-Au substrate, electrochemically-deposited Au nanoparticles, and the chemically-anchored AuNPs.

The current results in this paper confirmed strongly the good electrical communication of the AuNPs with the underlying electrode surface, and further proved the electrocatalytic behavior of AuNPs towards the oxygen reduction reaction. In addition, serving the alternative AuNPs' layers as a renewed activated-electrode surface is a new finding, that will definitely open the doors for further applications in the electrochemical catalysis. Furthermore, our fabrication scheme for the three-dimensional AuNPs self-assembly film with the smooth electron transfer and controlled layer' thickness can be utilized in the molecular devices development.

Conclusion

We have demonstrated the fabrication of AuNPs' multilayers arrays which were assembled onto different Au substrates using BDMT as a binder. The formation of repeatedly uniform AuNPs' layers with average monolayer thickness of about 5.5 nm was confirmed using TEM iamging and the necessity of the BDMT for the multilayer formation has been verfied by the XPS measurements. The AuNPs' layers immobilized on mercapto-terminated self-assemblies of BDMT achieved good electrical communication with the underlying electrode surface, and further, worked as a renewed activated-electrode surface. This AuNPs' layers showed a good electrocatalytic activity towards oxygen reduction (100 mV positive shift) and efficiently restored the catalytic activity that was entirely inhibited by the preceding BDMT layer. The aggregation phenomenon of the AuNPs during their assembly has been investigated and was found to depend, among other factors, on the substrate geometry and roughness.

Acknowledgements: The present work was financially supported by Grant-in-aids for Scientific Research (No. 12875164) and Scientific Research (A) (No. 19206079) to T. Ohsaka, from the Ministry of Education, Culture, Sports, Science and Technology (MEXT), Japan. A.I.A acknowledges a MEXT scholarship from the Japanese Governmant. M. S. El-Deab thanks the Japan Society for the promotion of Science (JSPS) for the invitaion fellowship.

[1] A. I. Abdelrahman, A. M. Mohammad, T. Okajima, T. Ohsaka, *J. Phys. Chem. B* **2006**, *110*, 2798.
[2] L. Wang, J. Bai, P. Huang, H. Wang, L. Zhang, Y. Zhao, *Electrochem. Commun.* **2006**, *8*, 1035.
[3] A. P. Alivisatos, *Science* **1996**, *271*, 933.
[4] A. P. Alivisatos, K. P. Johnsson, X. Peng, T. E. Wilson, C. J. Loweth, M. P. Bruchez, Jr., P. G. Schultz, *Nature* **1996**, *382*, 609.
[5] D. G. Schultz, X.-M. Lin, D. Li, J. Gebhardt, M. Meron, J. Viccaro, B. Lin, *J. Phys. Chem. B* **2006**, *110*, 24522.
[6] M.-C. Daniel, D. Astruc, *Chem. Rev.* **2004**, *104*, 293.
[7] R. Zanella, A. Sandoval, P. Santiago, V. A. Basiuk, J. M. Saniger, *J. Phys. Chem. B* **2006**, *110*, 8559.
[8] C. F. Vardeman, P. F. Conforti, M. M. Sprague, J. D. Gezelter, *J. Phys. Chem. B* **2005**, *109*, 16695.
[9] M. S. El- Deab, T. Ohsaka, *Electrochem. Commun.* **2002**, *4*, 288.
[10] J. H. Youk, M.-K. Park, J. Locklin, R. Advincula, J. Yang, J. Mays, *Langmuir* **2002**, *18*, 2455.
[11] R. G. Freeman, K. C. Grabar, K. J. Allison, R. M. Bright, J. A. Davis, A. P. Guthrie, M. B. Hommer, M. A. Jackson, P. C. Smith, D. G. Walter, M. J. Natan, *Science* **1995**, *267*, 1629.
[12] A. N. Shipway, E. Katz, I. Willner, *Chem. Phys. Chem* **2000**, *1*, 18.
[13] M. S. El-Deab, T. Ohsaka, *Electrochem. Commun.* **2002**, *4*, 288.
[14] T. Sagara, N. Kato, N. Nakashima, *J. Phys. Chem. B* **2002**, *106*, 1205.
[15] M. V. Tsodikov, T. N. Rostovshchikova, V. V. Smirnov, O. I. Kiseleva, Y. V. Maksimov, I. P. Suzdalev, V. N. Ikorskii, *Catalysis Today* **2005**, *105*, 634.
[16] C. R. Henry, *Appl. Surf. Sci.* **2000**, *164*, 252.
[17] Y. Wang, H. Liu, Y. Jiang, *J. Chem. Soc. Chem. Commun.* **1989**, 1878.
[18] Y. Wang, H. Liu, *Polymer Bull.* **1991**, *25*, 139.
[19] M. Brust, D. Bethell, D. Schiffrin, C. Kiely, *Adv. Mater.* **1995**, *7*, 795.
[20] M. Dorogi, J. Gomez, R. Osifchin, R. Andres, R. Reifenberger, *Phys. Rev. B* **1995**, *52*, 9071.
[21] G. Decher, *Science* **1997**, *277*, 1232.
[22] M. Sano, Y. Lvov, T. Kunitake, *Annu. Rev. Mater. Sci.* **1996**, *26*, 153.
[23] H.-L. Zhang, S. D. Evans, J. R. Henderson, *Adv. Mater.* **2003**, *15*, 531.
[24] C. Jiang, S. Markutsya, V. V. Tsukruk, *Langmuir* **2004**, *20*, 882.
[25] X. Zhou, C. Liu, Z. Zhang, L. Jiang, J. Li, *J. Colloid Interface Sci.* **2005**, *284*, 354.
[26] H. Zhang, H. Lu, N. Hu, *J. Phys. Chem. B* **2006**, *110*, 2171.
[27] L. Gao, E. Wang, Z. Kang, Y. Song, B. Mao, L. Xu, *J. Phys. Chem. B* **2005**, *109*, 16587.
[28] F. N. Crespilho, M. Emilia Ghica, M. Florescu, F. C. Nart, O. N. Oliveira, Jr., C. M. A. Brett, *Electrochem. Commun.* **2006**, *8*, 1665.
[29] M. Yang, Y. Yang, H. Yang, G. Shen, R. Yu, *Biomaterials* **2006**, *27*, 246.
[30] M. Olek, J. Ostrander, S. Jurga, H. Mohwald, N. Kotov, K. Kempa, M. Giersig, *Nano Lett.* **2004**, *4*, 1889.
[31] M. D. Musick, C. D. Keating, M. H. Keefe, M. J. Natan, *Chem. Mater.* **1997**, *9*, 1499.
[32] M. Brust, R. Etchenique, E. J. Calvo, G. J. Gordillo, *Chem. Commun.* **1996**, *16*, 1949.
[33] T. Baum, D. Bethell, M. Brust, D. J. Schiffrin, *Langmuir* **1999**, *15*, 866.
[34] C. R. Raj, A. I. Abdelrahman, T. Ohsaka, *Electrochem. Commun.* **2005**, *7*, 888.
[35] M. S. El-Deab, T. Sotomura, T. Ohsaka, *Electrochem. Commun.* **2005**, *7*, 29.
[36] M. S. El-Deab, T. Sotomura, T. Ohsaka, *J. Electrochem. Soc.* **2005**, *152*, C730.
[37] M. S. El-Deab, T. Sotomura, T. Ohsaka, *J. Electrochem. Soc.* **2005**, *152*, C1.

[38] K. R. Brown, D. G. Walter, M. J. Natan, *Chem. Mater.* **2000**, *12*, 306.
[39] K. V. G. K. Murty, M. Venkataramanan, T. Pradeep, *Langmuir* **1998**, *14*, 5446.
[40] B. Kim, S. J. Ahn, J. G. Park, S. H. Lee, Y. W. Park, E. E. B. Campbell, in *Proceedings of the Sixth International Conference on Nano-Molecular Electronics (ICNME 2004), Dec 15–17 2004, Vol. 499*, Elsevier, Amsterdam, 1000 AE, Netherlands, **2006**, pp. 196.
[41] D. G. Castner, K. Hinds, D. W. Grainger, *Langmuir* **1996**, *12*, 5083.
[42] C. Guarise, L. Pasquato, P. Scrimin, *Langmuir* **2005**, *21*, 5537.